J. metamorphic Geol., 2003, **21,** 241–252

Measurement and correlation of microstructures: the case of foliation intersection axes

A. R. STALLARD[1,*], K. A. HICKEY[1,†] AND G. J. UPTON[2]
[1]*School of Earth Sciences, James Cook University, Townsville 4811, Australia (a.stallard@geol.canterbury.ac.nz)*
[2]*Mathematics Institute, University of Essex, Colchester, UK*

ABSTRACT Recent studies have used the relative rotation axis of sigmoidal and spiral-shaped inclusion trails, known as Foliation Inflexion/Intersection Axis (FIA), to investigate geological processes such as fold mechanisms and porphyroblast growth. The geological usefulness of this method depends upon the accurate measurement of FIA orientations and correct correlation of temporally related FIAs. This paper uses new data from the Canton Schist to assess the variation in FIA orientations within and between samples, and evaluates criteria for correlating FIAs. For the first time, an entire data set of FIA measurements is published, and data are presented in a way that reflects the variation in FIA orientations within individual samples and provides an indication of the reliability of the data. Analysis of 61 FIA trends determined from the Canton Schist indicate a minimum intrasample range in FIA orientations of 30°. Three competing models are presented for correlation of these FIAs, and each of the models employ different correlation criteria. Correlation of FIAs in Model 1 is based on relative timing and textural criteria, while Model 2 uses relative timing, orientation and patterns of changing FIA orientations, and Model 3 uses relative timing and FIA orientation as correlation criteria. Importantly, the three models differ in the spread of FIA orientations within individual sets, and the number of sets distinguished in the data. Relative timing is the most reliable criterion for correlation, followed by textural criteria and patterns of changing FIA orientations from core to rim of porphyroblasts. It is proposed that within a set of temporally related FIAs, the typical spread of orientations involves clustering of data in a 60° range, but outliers occur at other orientations including near-normal to the peak distribution. Consequently, in populations of FIA data that contain a wide range of orientations, correlation on the basis of orientation is unreliable in the absence of additional criteria. The results of this study suggest that FIAs are best used as semiquantitative indicators of bulk trends rather than an exact measurement for the purpose of quantitative analyses.

Key words: Canton Schist; correlation; foliation intersection axes; porphyroblast.

INTRODUCTION

Compositional zoning within garnet porphyroblasts has long been used by metamorphic petrologists to reconstruct the *P–T* history of orogens (e.g. Selverstone *et al.*, 1984; Kohn *et al.*, 1992). Microstructures preserved as inclusion trails in porphyroblasts provide a record of the deformation history to compliment *P–T* calculations (e.g. Jones, 1994; Johnson, 1999). For this reason, porphyroblasts are increasingly recognised as recorders of progressive kinematic and metamorphic conditions during orogenesis.

Recent studies have proposed a method of quantifying microstructures preserved in porphyroblasts by determining the orientation of the axis to inclusion trail curvature, and this axis has been termed the Foliation Inflexion/Intersection Axis, or FIA (e.g. Hayward, 1990; Bell *et al.*, 1995; see also Powell & Treagus, 1967, 1970 and Rosenfeld, 1968 for earlier methods of measuring rotation axes in porphyroblasts). FIA orientations have been used as a tool to investigate a variety of geological topics, including fold mechanisms, porphyroblast rotation, shear sense, and timing of porphyroblast growth (e.g. Hayward, 1990; Davis, 1993; Bell *et al.*, 1995; Bell & Hickey, 1997). Essential elements of these studies are the interpretation and correlation of commonly complex inclusion trail geometries, measurement of FIA orientations, and partitioning of FIAs into temporally related sets. As the number of publications that report FIA data have grown, some workers (e.g. Johnson, 1999) have highlighted the following aspects of the FIA technique that require clarification:

(1) The FIA orientation is commonly determined from complex inclusion trails. How can the method be refined to minimise bias and yield reproducible results?
(2) FIA orientations are determined on the scale of a sample, yet variation in FIA orientations within a

* Now at: Department of Geological Sciences, University of Canterbury, Christchurch, New Zealand.
† Now at: Mineral Deposit Research Unit, Department of Earth and Ocean Sciences, University of British Columbia, Vancouver, BC V6T 1Z4, Canada.

sample may result from the curvature of a foliation around pre-existing porphyroblasts and contrasting FIA orientations within different porphyroblasts from the sample. What is the natural extent of this variation and how can it be expressed in the presentation of data?

(3) A sample may contain multiple FIAs from core to rim of porphyroblasts, and a population of samples may contain a number of temporally related sets of FIAs (e.g. Bell *et al.*, 1998). Recognising these patterns depends upon correlating inclusion trails within a sample, and FIAs between samples. How can this be reliably and objectively achieved?

This paper aims to address these questions using new FIA data from the Canton Schist, Georgia, USA. Numerous garnet porphyroblasts in the Canton Schist contain complex inclusion trail geometries that indicate the presence of multiple FIAs of different orientation from the core to rim of porphyroblasts. Methods of correlating inclusion trails and distinguishing temporally related FIA sets using criteria such as relative timing, orientation, and inclusion mineralogy and texture are applied to the Canton Schist. From this, the natural variation in FIA orientations at different scales is assessed, and implications for the FIA method are discussed.

METHOD OF FIA DETERMINATION

Use of inclusion trail asymmetry

The most accurate method to determine FIA orientations is reconstruction of the 3D inclusion trail geometry in individual porphyroblasts by such means as computed X-ray tomography or serial sectioning and computer-aided reconstruction. However, we are unaware of any present tomography technique that can produce the resolution required for such a study, and reconstruction of the trail geometry from serial sections is a time-intensive and difficult procedure, of which the greatest problem is correlating individual inclusion surfaces from one serial thin section to the next (see Schoneveld, 1979; Johnson, 1993).

In the absence of 3D imaging or reconstructions, Hayward (1990), Bell *et al.* (1995, 1998) and Bell & Hickey (1997) have described a method by which FIA orientations can be constrained from a population of porphyroblasts within a single oriented rock sample (Fig. 1). FIA trends (0–180°) are determined by recording the asymmetry of inclusion trail curvatures in a regular fan of oriented vertical thin sections. This usually requires between 10 and 14 thin sections per sample (typically at 10–20° intervals). The orientation of the FIA is indicated by a change in the asymmetry of inclusion trail curvature (e.g. from clockwise to anticlockwise) recorded in thin sections oriented either side of the FIA (Fig. 1; see also Bell *et al.*, 1998 for a full outline of the technique). Experience has shown that in some porphyroblasts, particularly garnet, the axis of inclusion trail curvature undergoes a change in orientation from core to rim (Hayward, 1990; Bell & Hickey, 1997; Bell *et al.*, 1998; Hickey & Bell, 1999). This geometry causes different parts of the inclusion trails to change asymmetry at different orientations (see below). Bell *et al.* (1998) termed these multi-FIA samples to distinguish them from single-FIA samples where the axis of inclusion trail curvature within porphyroblasts maintains a near constant orientation from core to rim.

The plunge of a FIA can be found in the same way using variably dipping thin sections that strike parallel to the trend. The total accumulated error in determining the trend or plunge of an FIA in this way has been estimated at ± 8° (Bell & Hickey, 1997). This figure represents the potential errors involved in compass measurements, repositioning of the sample in the laboratory, and preparation of oriented thin sections.

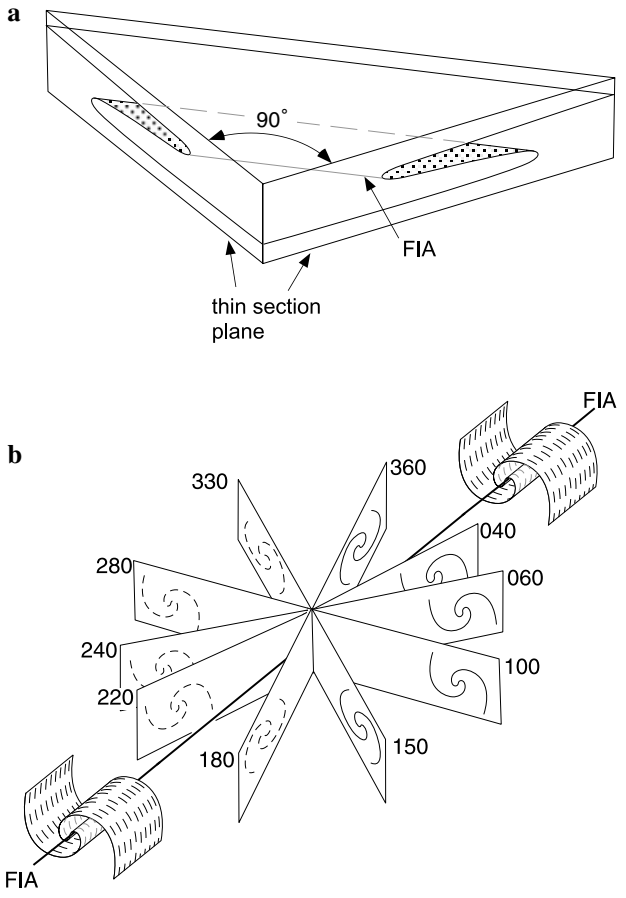

Fig. 1. 3D sketches showing the method used to determine a FIA trend. (a) The asymmetry of the inclusion trail curvature switches when viewed either side of the FIA trend (compare Z-shaped geometry on LHS of block diagram with S-shape on RHS). (b) Sketch illustrating the range of inclusion trail geometries expected in thin sections of varying orientation about a single FIA. The spiral surfaces marked on the thin sections represent the geometry of the inclusion trail surface within the porphyroblast. Five thin sections of varying strike are shown. The inclusion trail geometry observed in each thin section is sketched onto the thin section. Dashed lines indicate that the geometry is viewed from the opposite direction to that indicated by solid lines. Note that the asymmetry of the inclusion trail curvature changes either side of the FIA. This allows the FIA trend to be determined by examining multiple vertical thin sections at, for example, 20° intervals. Thin sections must be viewed in the same direction when comparing inclusion trail asymmetries. Modified from Bell *et al.* (1998).

Limitations and pitfalls of FIA determination

In contrast to serial sectioning and X-ray tomography techniques, the method of FIA determination described above results in a FIA orientation on the scale of a sample, and uses inclusion trail curvature from many porphyroblasts within the sample. It does not represent a unique physical feature and consequently is not a

quantitative measure. The successful application of this method is dependent on FIAs within individual porphyroblasts being non-randomly oriented, and having a restricted range in orientation within a sample, as otherwise both anticlockwise and clockwise inclusion trail asymmetries would be recorded in every thin section and the method would be unworkable. Conversely, if all the FIAs within a sample were linear and trending, for example, 090°, then all the inclusion trail asymmetries would switch (e.g. from clockwise to anticlockwise) between thin sections oriented either side of the FIA at $<090°$ and $>090°$, and individual thin sections would contain either all clockwise or all anticlockwise inclusion trail curvatures.

In practice, rocks have geometries intermediate between these two scenarios, as it is common to find both anticlockwise and clockwise asymmetries within thin sections oriented close to the FIA (e.g. Fig. 2; Hayward, 1990). This reflects the curvilinear geometry of FIAs within individual porphyroblasts (Hayward, 1990), and variation in orientation between porphyroblasts within the sample. Due to this intrasample variation in orientation, the switch in asymmetry defining the FIA occurs over an angular range rather than at a discrete point (see also Hayward, 1990; Bell *et al.*, 1998). For this reason, FIA data presented as a discrete orientation (e.g. 080°; cf. Bell *et al.*, 1998) do not adequately reflect the 3D complexity of inclusion trails and the nonlinear nature of FIAs, and data presented in this way are probably not reproducible.

This issue is compounded by the difficulties in minimising bias in the determination of FIAs, as the method requires intensive interpretation and correlation of microstructures. These problems can be addressed in part by the use of an asymmetry plot (Fig. 2) to present more data than simply the discrete FIA orientation. An asymmetry plot shows the total numbers of clockwise and anticlockwise asymmetries measured in thin sections of different orientations. These are the raw data used to determine the FIA orientation and to assess the amount of variation in FIA orientations within a sample (see Table S3 for raw data from Canton Schist samples). Asymmetry plots also have the advantage of showing how many porphyroblasts were used to constrain the FIA orientation.

A second way in which complexities in the inclusion trails can be represented in the data is by indicating the FIA orientation as a mid-point value and interval over which the asymmetry switches (e.g. 080 ± 20°). This indicates the spread of FIA orientations within and between porphyroblasts in a sample. As an extension of this idea, we have developed a new statistical procedure to determine the FIA trend orientation from the data recorded in asymmetry plots. This technique, based on maximum likelihood estimation (e.g. Edwards, 1972), estimates the range in FIA trends within a sample and calculates a FIA orientation based upon the entire population of sampled garnet.

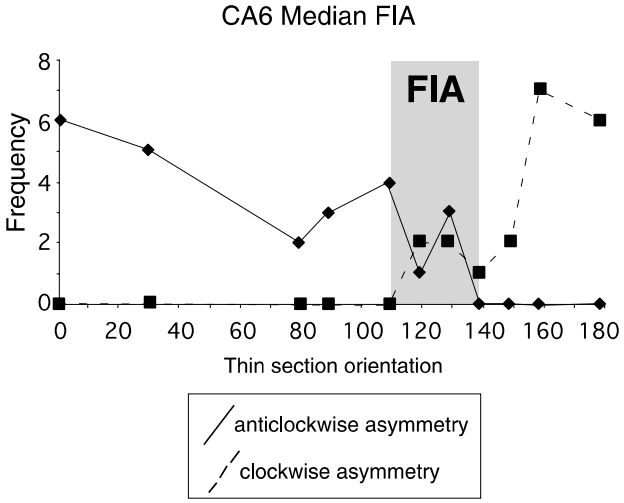

Fig. 2. The asymmetry plot shows the distribution of inclusion trail asymmetries in different thin sections from sample CA6 (median FIA). The trend of the FIA is located at the switch in asymmetry (grey shading).

A statistical approach to FIA determination within single samples—a Maximum Likelihood Procedure

The method of determining a FIA trend, shown in Fig. 1, involves recording the asymmetry of inclusion trail curvature in a series of vertical thin sections cut at 10–20° intervals around the compass (Bell *et al.*, 1995). If the inclusion trail asymmetry changes over a narrow angular range, there is little doubt concerning the orientation of the FIA. However, as mentioned above, the change in asymmetry may occur over a large angular range and, confusingly, there can sometimes be multiple apparent flips within a single sample. The new statistical procedure allows for these various possibilities.

The model is based on relating the dependence of p, the proportion of asymmetries that are clockwise-oriented, on θ the orientation of the section. The objective is to estimate μ, the FIA orientation. The model proposed is the logistic model

$$\log\{p/(1-p)\} = \beta \sin(\theta - \mu)$$

The quantity $\log\{p/(1-p)\}$ is equal to 0 if $p = 0.5$, which is the probability of interest. The quantity $\sin(\theta - \mu)$ is equal to 0 when $\theta = \mu$. Thus μ is the FIA orientation. The parameter β controls the speed of the change between clockwise and anticlockwise, with $\beta = \infty$ corresponding to a precipitate change and a near-zero value of β corresponding to a very slow change.

Suppose that there are r_i clockwise-oriented trails out of the n_i trails at orientation i. Let p_i (β, μ) be the model probability. The kernel of the likelihood for a rock with observations in 18 orientations is L (β, μ), given by

$$L(\beta, \mu) = \prod_{i=1}^{18} p_i(\beta, \mu)^{r_i} \{1 - p_i(\beta, \mu)\}^{n_i - r_i}.$$

Maximization of L (β, μ) is easily performed by enumeration with double-precision calculations. We denote the maximum value by $L_{\max}$ and the corresponding parameter values by $\hat{\beta}$ and $\hat{\mu}$.

To obtain a confidence interval for μ (β is of no direct interest), we note that the hypothesis $\mu = \mu_0$ would be accepted using a likelihood-ratio test, provided the value of

$$\min_{\beta}\{L_{\max} - L(\beta, \mu_0)\}$$

is not too large. For a test at the $100\alpha\%$ significance level, the appropriate value is the upper $100\alpha\%$ point of a chi-squared distribution with 1 degree of freedom. We can use this result to identify the smallest and largest values of μ_0 for which the hypothesis would be accepted, and these values define an approximate two-sided $100\alpha\%$ confidence interval for μ.

In general, confidence intervals found in this way will not be symmetric about $\hat{\mu}$. The intervals will be narrowest where there is a single flip and, at each orientation, r_i is equal to either n_i or 0. In such cases $\hat{\beta} = \infty$.

The data include several cases of multiple flips. In these cases, in which the model does not fit the data so well, the goodness of fit can be assessed by a second likelihood-ratio test, with a product-binomial comparison. However, in every case the fit proved acceptable.

Tables S1, S2 and S3 contain FIA characteristics and raw counts of inclusion trail asymmetry in thin sections of Canton Schist. These are available online from http://www.blackwellpublishing.com/products/journals/suppmat/JMG/JMG439/JMG439sm.htm.

FIAS IN THE CANTON SCHIST

Garnet porphyroblast microstructures

For this study, 25 samples of the Canton Schist were collected along a 45-km section north of Atlanta, Georgia (Fig. 3). The Canton Schist is a quartz-mica schist deformed and metamorphosed during the middle Palaeozoic (Dallmeyer, 1978). The geology of the sample area and the microstructure of the matrix and garnet porphyroblasts have been described in detail by Stallard & Hickey (2001). Garnet occurs as subspherical porphyroblasts 4–8 mm in size and contains prominent inclusion trails of quartz, ilmenite, graphite and muscovite. Textural criteria were used to distinguish cores and rims within the porphyroblasts (e.g. Fig. 4a) in all but one sample (sample CA10, see below). Porphyroblast cores are characterised by a high density of quartz inclusions, while rims contain sparsely distributed inclusions of predominantly ilmenite, graphite and muscovite. Use of the terms core and rim in the following text refer to this textural division (see Stallard & Hickey, 2001 for more detailed description of these textures). The core-rim transition is also marked by a tight curvature of inclusion trails (e.g. Fig. 4a) similar to the deflection surfaces described by Passchier & Trouw (1996).

Inclusion trails in the porphyroblast cores are generally subplanar inclined surfaces that curve into subplanar and subhorizontal trails in the outer core. Rim

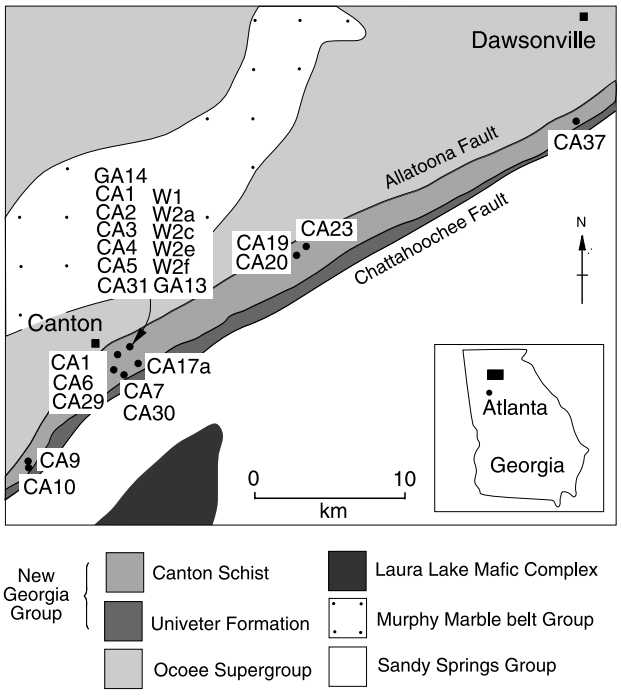

Fig. 3. Sample localities and simplified regional geology of the Canton area. Geology after McConnell & Abrams (1984).

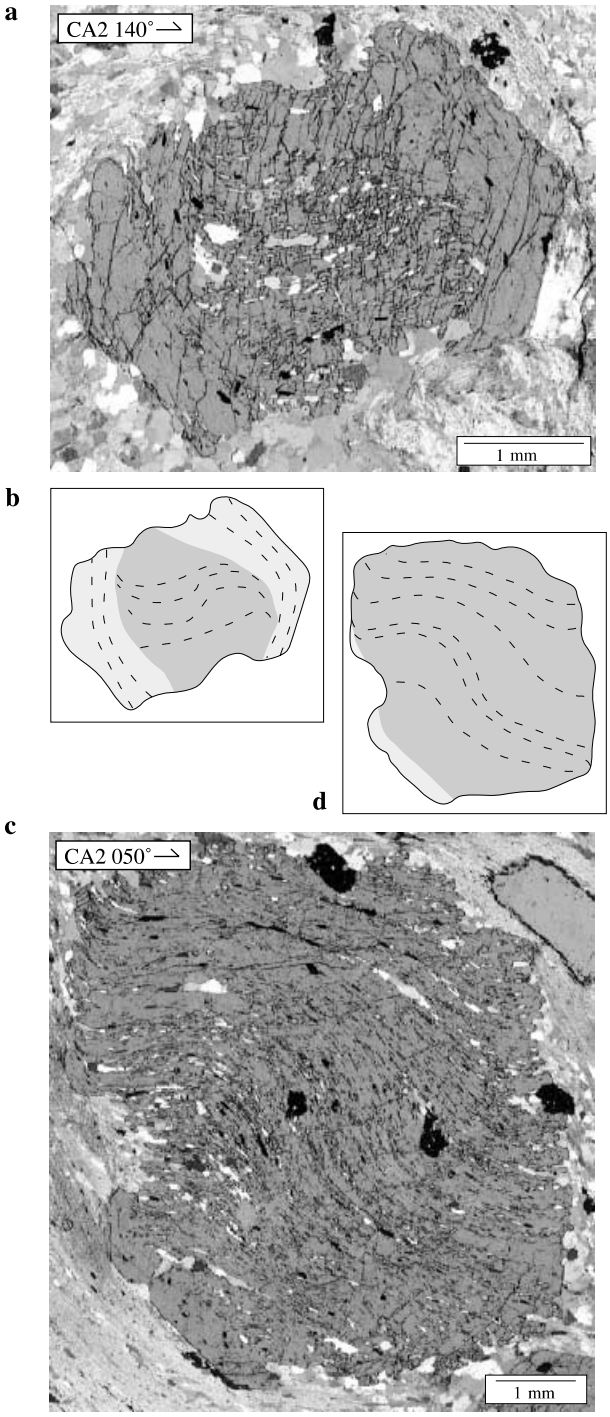

Fig. 4. Example of contrasting inclusion trail geometries in a sample that contains both spiral-shaped (a) and staircase (c) geometries in thin sections of different orientation. (b) and (d) are line diagrams of the accompanying photomicrographs. The inclusion trail curvature in the core of the porphyroblast is different in the two porphyroblasts, but the curvature into the rim is clockwise in both, indicating rotation axes of different orientation for the core and rim curvatures. Dark and light grey shading on line diagrams indicates textural cores and rims, respectively. Vertical thin sections, sample number and strike of section shown in top left corner.

trails are gently curved to subplanar, and commonly continuous with the matrix foliation. Sample CA10 contains small garnet typically < 2 mm diameter, with comparable inclusion trail geometries to other samples but without textural cores and rims.

FIA trend data

More than 400 oriented thin sections were prepared to determine FIA trends for the 25 samples of Canton Schist. Asymmetry data (Table S3) recorded from inclusion trails were used to determine FIA trends using the statistical method outlined above. The total number of porphyroblasts intersected by thin sections from four randomly chosen samples was between 52 and 70, and asymmetry measurements were recorded from between 45 and 70% of the intersected porphyroblasts within each sample. Factors that prevented measurement of inclusion trail asymmetry within individual porphyroblasts include a lack of inclusion trails, intersection of section with porphyroblast rim only, lack of porphyroblast rim growth, and trail geometries that were either linear or finely crenulated.

A total of 61 FIA trends were determined (Table S1; Fig. 5). Fourteen samples contain multiple reversals of inclusion trail curvature from core to rim within individual porphyroblasts, and this enabled three distinct FIA trends of known relative age to be determined in these samples. Multiple FIAs preserved from core to rim within individual porphyroblasts are labelled core, median and rim FIAs, respectively, reflecting the relative timing of each FIA within the porphyroblast. Significantly, no sample contained more than one interval of curvature, or a reversal in asymmetry, within each of the textural defined zones of inclusion trail curvature defined above. Rim growth has not occurred in all garnet porphyroblasts, and ten samples contained insufficient rims preserving the rim-matrix inclusion trail curvature to determine the rim FIA. In these samples, two FIAs have been determined (core and median). Similarly, due to the inconsistent development of rims in certain samples, and lack of preservation of curvature at the core-rim transition, a single core FIA only was determined in three samples (CA 19, 20, 23).

The trend orientations are widely distributed, although the majority of data are clustered between 030° and 130° (Fig. 5a). FIAs in the textural core of the porphyroblasts have a general ENE trend. FIAs defined by curved inclusion trails at the core–rim boundary have a wide range of trends with an ESE directed modal peak. Rim FIAs are dominantly oriented E–W. A number of FIA orientations have large angular intervals at the 95% confidence level, and this reflects the presence of thin sections containing anomalous asymmetries (e.g. Table S3, sample CA2 median FIA). These symmetry reversals may reflect a local switch in asymmetry across a microscale fold hinge or heterogeneous rotation of porphyroblasts.

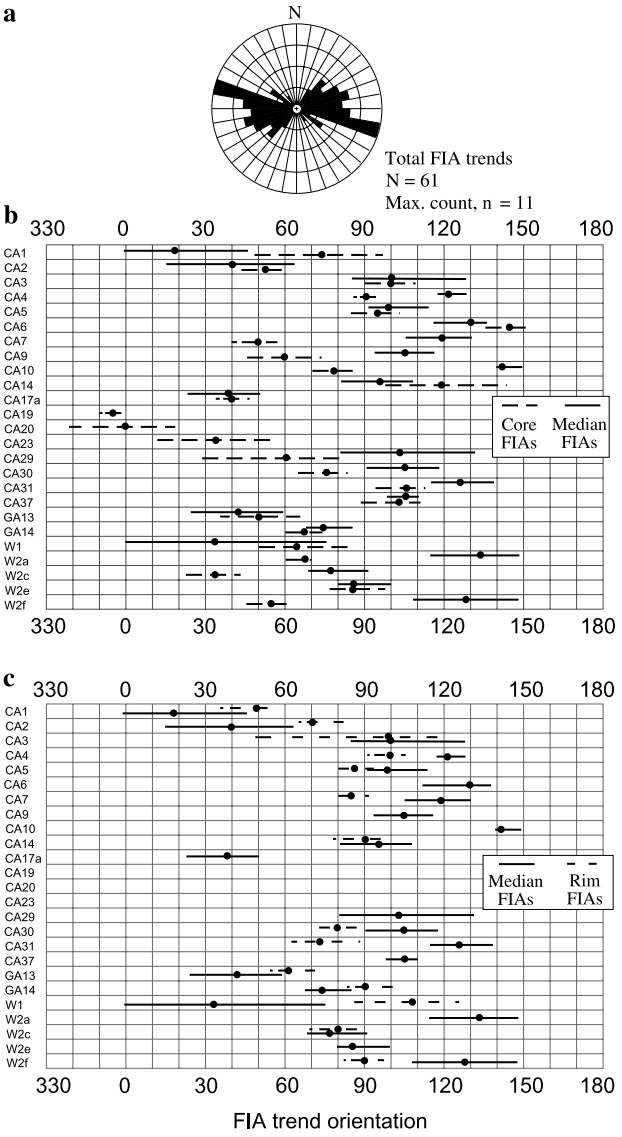

Fig. 5. (a) Distribution of total Canton Schist FIA trend midpoints. (b, c) Plots showing the distribution of core, median and rim FIA trends. Median FIAs are repeated in both plots to allow comparison between the orientation of successive FIAs within each sample. Black bars indicate the 95% confidence interval for the FIA estimate as calculated using the statistical model described in the text.

It is also possible that these reversals reflect some natural spread in FIA trend within samples.

An estimate of FIA plunge was made for 31 of the 61 FIA trends. Sections used to determine plunges were radially oriented at horizontal, −20°, −40°, −90°, + 20°, + 40° and + 90° dip in the direction of the FIA trend. Plunge measurements are less tightly constrained than the trends, as the plunge could not be constrained further due to insufficient sample. Twenty-two samples have a FIA plunge of <40°, while three samples have a plunge between 40° and 90°, and six samples have poorly constrained plunges of between

20° and 90° (Table S1). The following discussions focus on FIA trends rather than plunges, as trend data are available for more samples, and are better constrained by oriented thin sections at 10° intervals close to the FIA.

Variation in FIA trends within samples

The occurrence of both clockwise and anticlockwise asymmetries in thin sections oriented close to the FIA indicates a spread in FIA orientations within individual samples (e.g. Fig. 2). This reflects the nonlinear geometry of FIAs (Powell & Treagus, 1967; Hayward, 1990), as well as variation in orientation between different porphyroblasts (Johnson, 1999), and is distinct from errors accrued during measurement.

In the Canton Schist, the average amount of intrasample spread in FIA trend can be estimated by calculating the range over which both anticlockwise and clockwise asymmetries are recorded close to the FIA. These values, derived from the asymmetry data presented in Table S1, are ± 9° for core FIAs, ± 14° for median FIAs and ± 10° for rim FIAs. The statistical analysis produces 95% confidence intervals for the orientation of core, median and rim FIAs of 23°, 29° and 23°, respectively. These estimates of intrasample FIA spread are likely to underestimate the true spread however, as they are limited by the sample size of recorded asymmetries relative to the total population.

The true spread in FIA orientations can be determined only if the 3D geometry of inclusion trails in all porphyroblasts from the sample can be quantified. The intrasample range of FIA orientations in Canton Schist samples is therefore greater than those recorded in Table S1, and minimum values of 30° are proposed as being more representative of intrasample spread. If all porphyroblasts in a sample were to be analysed, the reversal in inclusion trail asymmetry coincident with the FIA trend would likely occur over a 30–50° interval rather than abruptly over a narrow interval.

IDENTIFYING TEMPORALLY RELATED SETS OF FIAS IN THE CANTON SCHIST

An important part of making geologically meaningful interpretations of FIA data is correlating temporally related FIAs and determining the relative timing of sets of coeval FIAs (e.g. Bell & Hickey, 1997; Bell *et al.*, 1998). A set is defined as those FIAs that formed at the same time in the geological history. In the absence of absolute dating techniques, the relative timing provided by porphyroblasts that record multiple FIA orientations from core to rim is the key to identifying different sets. Relative timing can also be assessed by the relationship of the inclusion trails to other porphyroblast and matrix microstructures, or the growth history of the porphyroblast defined by inclusion texture and mineralogy and chemical criteria. FIA orientation has previously been used as a criterion for correlating FIAs and distinguishing different sets (e.g. Bell *et al.*, 1998), but the validity of this approach depends upon knowledge of the limits of spatial variation in FIA orientations within a temporally related set (see Bell *et al.*, 1998 and Davis, 1993 for contrasting views on this topic).

Within the Canton Schist, seven samples contain core, median and rim FIAs of contrasting orientations (e.g. sample CA7 in Table S1), and this indicates a minimum of three sets within the population. However, further partitioning of the data into sets depends on the criteria used to correlate FIAs between samples. To illustrate this point, we present three contrasting analyses of the FIA data, each of which partitions the data into sets according to different criteria. In Model 1, FIAs are correlated using inclusion trail textures and timing relative to other FIAs, while Model 2 uses FIA orientation, timing relative to other FIAs, and patterns of changing FIA orientations, and Model 3 employs FIA orientation and timing relative to other FIAs as correlation criteria. Each of the three models is consistent with the relative timing criteria indicated by multi-FIA samples, but important differences in each model result from the choice of criteria used to correlate the FIAs.

Model 1. Correlation of FIAs using relative timing and textural criteria

FIAs are correlated on the basis of inclusion trail textures and timing relative to other FIAs (e.g. the rim FIA obtained from a sample must be placed in a set that is younger than any set containing the core FIA from that same sample), independent of FIA orientation. This involves the interpretation that the deflection plane of inclusion trails at the core–rim boundary (Fig. 4a) formed in the same deformation event in all samples. Accordingly, the population of FIAs is partitioned into three sets (Fig. 6). Set 1 contains FIAs that are preserved in porphyroblast cores (those listed as Core FIAs in Table S1), Set 2 is comprised of FIAs that coincide with the core–rim boundary (listed as median FIAs in Table S1), and Set 3 contains those FIAs that are preserved in porphyroblast rims (listed as rim FIAs in Table S1). FIAs from sample CA10 are correlated using core-to-rim relative timing only, due to the absence of textural cores and rims. Within each of the three sets, data are concentrated within a 20–60° interval, with smaller numbers of FIAs having other orientations including some orthogonal to the main cluster of data (Fig. 6). We tested for differences in the orientation of each set using a two-sample bootstrap test (see Chapter 8 of Fisher, 1993) and found that the total Set 1 FIAs and total Set 2 FIAs differ in orientation at the 0.1% significance level and the total Set 2 and total Set 3 FIAs also differ at the 0.1% significance level. There is a bulk clockwise shift in FIA trend between Set 1 and Set 2, and a bulk anticlockwise shift from Set 2 to Set 3.

a

	Set 1 (core FIAs)	Set 2 (med. FIAs)	Set 3 (rim FIAs)
CA1	074	019	049
CA2	053	040	071
CA3	100	100	100
CA4	091	122	099
CA5	095	102	086
CA6	144	127	
CA7	050	119	085
CA9	060	105	
CA10	078	142	
CA14	119	096	090
CA17a	040	039	
CA19	175		
CA20	000		
CA23	034		
CA29	060	103	
CA30	075	105	080
CA31	105	125	073
CA37	104	105	
GA13	050	042	061
GA14	066	075	090
W1	066	043	108
W2a	066	134	
W2c	033	077	080
W2e	085	086	
W2f	054	128	090

b

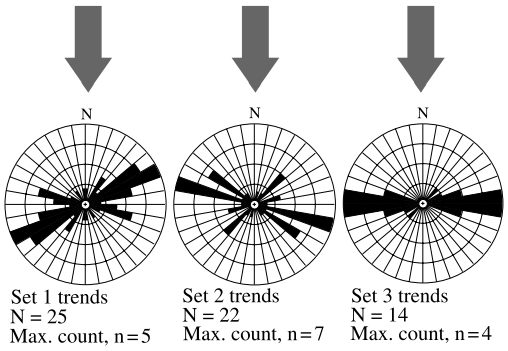

Fig. 6. Division of the FIA data into temporally related sets using relative timing and textural criteria to correlate FIAs. The data are shown tabulated (a), and as trend mid-point orientations on rose diagrams (b).

Model 2. Correlation of FIAs using orientation, relative timing and patterns of changing FIA orientation

In Models 2 and 3 (see below), FIAs are correlated based upon timing relative to other FIAs (for multi-FIA samples) and FIA orientation, independent of inclusion trail textures. Accordingly, FIAs are defined only where a reversal in inclusion trail asymmetry occurs, as equivalent inclusion trail curvatures are not identified in different thin sections. Because FIAs are defined at reversals in asymmetry, temporally distinct but comparably oriented FIAs within a sample (e.g. sample CA3, Table S1) are recorded as a single FIA (cf. texturally based method described above, in which FIAs are determined at each zone of curvature, regardless of asymmetry or orientation). This method of determining FIAs has been used in previous studies by Bell & Hickey (1997), Bell *et al.* (1998), and Hickey & Bell (1999). An analysis of Canton Schist data using this method is shown in Table S2 and Fig. 7. The bulk distribution of FIAs produced by the two methods (i.e. Model 1 *cf.* Models 2 & 3) is comparable (compare Figs 5a & 7a), but Fig. 7(a) contains fewer data, as successive FIAs of comparable orientation in Fig. 5(a) are recorded as the same FIA in Fig. 7(a).

In Model 2 (Fig. 8), FIAs are correlated using relative timing, orientation, and patterns of changing FIA orientations from core to rim. The most distinctive pattern of changing FIA trends in multi-FIA samples is the consistent (12 of 16 samples record this trend) clockwise shift between core and median FIAs (Fig. 7c). This shift averages 46° (6 of the 12 measurements are between 25° and 55°, and the total spread is from 14° to 74°), and is used as a basis for distinguishing the first two FIA sets (Fig. 8). Set 1 contains all those core FIAs from samples that record a clockwise shift between core and median FIAs, and Set 2 contains all those median FIAs from samples recording the same shift.

Samples CA1, CA2, CA5 and CA14 are exceptions to the above pattern. The median FIAs in these samples, as well as the rim FIAs from multi-FIA samples, are partitioned into two further sets (Sets 3 & 4). Set 3 contains the north- and northeast-trending data and includes the median FIAs from samples CA1 and CA2 (Fig. 8a). Set 4 contains FIAs oriented approximately east–west, and includes all rim FIAs and the median FIA from sample CA14. Data from single-FIA samples are partitioned between the four sets on the basis of orientation. The resulting four sets are in agreement with the relative timing recorded in multi-FIA samples and preserve the consistent shift in orientation between core and median FIAs (Sets 1 & 2). Samples that don't record the clockwise shift are partitioned into Sets 3 and 4. The resulting angular spread of orientations within each set in smaller than that in Model 1.

Model 3. Correlation of FIAs using relative timing and FIA orientation alone

In Model 3, FIAs are correlated using relative timing and FIA orientation only. As in Model 2, successive FIAs of comparable orientation are treated as a single FIA, and accordingly, the data shown in Table S2 are used for analysis (*cf.* data in Table 1S). In this model FIAs are correlated on the basis of orientation, and therefore assume that temporally related FIAs have similar orientations in all samples. On this basis, the data are divided into four sets (Fig. 9). Three sets are initially determined at 170°–049°, 050°–089° and 090°–140° by equating peaks in the total distribution (see Fig. 7a,b) with individual sets. To remain consistent with the relative timing of successive FIAs in multi-FIA samples (e.g. CA1 & CA9), the relative timing of the three sets is as follows: the set with orientations from 050°–089° is

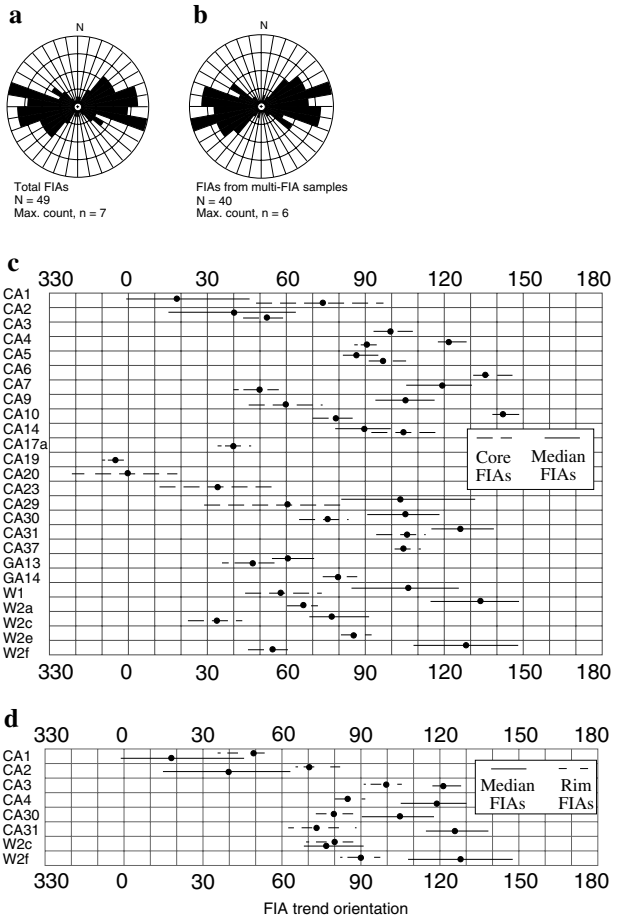

Fig. 7. Canton Schist FIA data determined on the basis of orientation and relative timing, independent of textural criteria. (a) Distribution of FIA trend mid-points from all samples. (b) FIA trend mid-points from multi-FIA samples only. (c, d) Plots showing the distribution of core, median and rim FIA trends. Black bars indicate the 95% confidence interval for the FIA estimate as calculated using the statistical model described in the text.

a

	Set 1 (consistent CW shift to Set 2)	Set 2 (consistent CW shift from Set 1)	Set 3 (N & NE FIAs)	Set 4 (late FIAs)
CA1	074		019	049
CA2	053		040	071
CA3		100		
CA4	091	122		099
CA5	098			086
CA6		135		
CA7	050	119		085
CA9	060	105		
CA10	078	142		
CA14		111		090
CA17a			040	
CA19a			175	
CA21			000	
CA23			034	
CA29	060	103		
CA30	075	105		080
CA31	105	125		073
CA37		105		
GA13	047	061		
GA14	080			
W1	058	108		
W2a	066	134		
W2c	033	077		080
W2e	085			
W2f	054	128		090

b

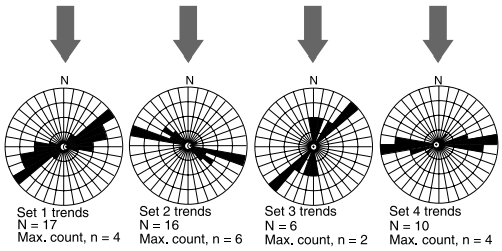

Fig. 8. Division of the FIA data (see Table S2) into temporally related sets using relative timing, orientation and patterns of shifting FIA orientations to correlate FIAs. The data are shown tabulated (a), and as trend mid-point orientations on rose diagrams (b).

earliest (Set 1), followed by the set with orientations from 090°–140° (Set 2), and the set with orientations from 170°–049° (Set 3). However, it is impossible to both accommodate all the data into these three sets and preserve the relative timing of multi-FIA samples. For example, sample CA7 contains three FIAs oriented at 050° (earliest), 119° (median) and 085° (youngest; Fig. 9a). The earliest FIA (050°) is consistent with inclusion in Set 1 (Fig. 9b), and the median FIA is placed in Set 2 with other FIAs in the 090°–140° orientation range, but the youngest FIA (085°) cannot be placed into Set 3, as it is not oriented in the 170–049° range. Therefore it is necessary to establish a fourth set (Set 4), which contains late-stage FIAs oriented in a range from 049°–120° (Fig. 9). The four sets contain FIAs with a similar distribution to those in Model 2, but with a smaller spread in orientations within each set.

A comparison of the three models

Despite the contrasting methods of correlation used in each model, certain patterns in the partitioning of FIAs are common to all three models, and these patterns provide a minimum interpretation of the data. Three main FIA sets are recognised, and each model shows the same relative timing between the sets. The earliest set contains data that cluster between 050° and 080°, with a peak concentration at *c*. 060°. FIAs in the second set cluster between 090° and 150°, and data in the youngest set are concentrated between 070° and 100°, with a peak at *c*. 095° (note that this latter set equates to Set 4 in Models 2 and 3). There is a bulk clockwise shift in FIA orientation from the first to second sets, and a bulk anticlockwise shift from the second to third sets.

Despite these similarities, two principal differences distinguish the three models. First, Model 1 has 3 sets, whereas Models 2 and 3 have an additional set accommodating north and north-east trending data. Second, the spread in orientations within individual sets is greater in Model 2 than Model 3, and greater again in Model 1 than Model 2. These differences result from contrasting interpretations of outliers in

a

	Set 1 (050°–089°)	Set 2 (090°–140°)	Set 3 (170°–049°)	Set 4 (049°–120°)
CA1	074		019	049
CA2	053		040	
CA3		100		
CA4		091, 122, 099		
CA5		098		086
CA6		136		
CA7	050	119		085
CA9	060	105		
CA10	078	142		
CA14		111, 90		
CA17a			040	
CA19a			175	
CA21			000	
CA23			034	
CA29	060	103		
CA30	075	105		080
CA31		105, 125		073
CA37		105		
GA13			047	061
GA14	080			
W1	058	108		
W2a	066	134		
W2c			033	077, 080
W2e	085			
W2f	054	128		090

b

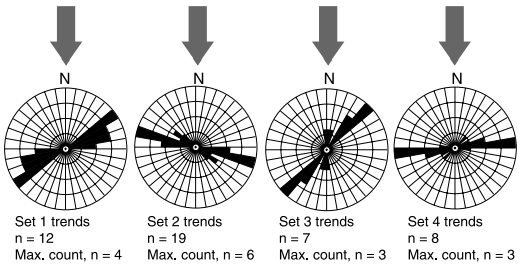

Fig. 9. Division of the FIA data (see Table S2) into temporally related sets using relative timing and FIA orientations to correlate FIAs, independent of textural criteria. Note that although core FIAs from some samples are correlated with rim FIAs from others, the relative timing indicated by the multi-FIA data (Table S2) is still preserved. The data are shown tabulated (a), and as trend mid-point orientations on rose diagrams (b).

the data set (e.g. north- and northeast trending FIAs in Model 1, *cf.* Model 3). The outliers can be interpreted either as FIAs that formed at a different time to the main concentration of FIA trends, and necessitating a separate set (e.g. Models 2 & 3), or as reflecting the natural spread in orientation of a population of time-equivalent FIAs (e.g. Model 1). Deciding which of the alternative interpretations (i.e. Models 1, 2 or 3) best describes the data rests upon the validity of the different correlation criteria and an understanding of the natural spread in orientation of temporally related FIAs. These topics are considered further below.

DISCUSSION

Correlating FIAs and determining FIA sets

The interpretation of FIA data involves correlating inclusion trail curvatures within a sample to determine FIA orientations, and correlating FIA orientations between samples to distinguish temporally related sets. The most reliable criterion for correlating inclusion trails and FIAs is timing relative to other microstructures or distinctive textural patterns from the core to the rim of porphyroblasts. Orientation can only be used as a criterion for correlating FIAs if the population of data has a restricted range, or if the data consist of several concentrations without overlap. The use of orientation as a criterion assumes that FIAs which formed at the same time have a similar orientation and that original orientations are unaffected by younger deformation.

Many factors can contribute to variation in the orientation of coeval FIAs. These include the heterogeneous rheology of the crust, rotation of the kinematic reference frame, the anastomosing of foliations around inhomogeneities such as granitic bodies, and rotation of porphyroblasts relative to other porphyroblasts in the rock mass. It is possible that a population of FIA data will show similar variation in orientations to that recorded in a population of foliation or fold axis measurements. Davis (1993) described FIAs of widely varying orientation around a granitic body, but other studies have described FIA data from multiply deformed terranes with minimal variation of orientations (e.g. Bell & Hickey, 1997). The three models of partitioning Canton Schist FIA data presented earlier (Figs 6, 8 & 9) show a clustering of data. In Model 1, 75% of FIAs are grouped within a 60° interval, while in Models 2 and 3, 92% and 100%, respectively, are grouped within a 60° interval. The maximum spread within sets in each model is 147° in Model 1, 81° in Model 2 and 52° in Model 3. At any point in time FIAs form over angular range, and this angular range may rotate with time. Also, it is possible that textural zone contacts are not time equivalent across samples and that there is some overlap of core and rim growth in different samples. Given this, and the natural variation in the orientations of geological structures (see above; also Davis, 1993), it is probable that within a set of temporally related FIAs, the majority of data (> 75% in the case of the Canton Schist) will cluster within a 60° range, although smaller numbers of data may exist at other orientations, including close to orthogonal to the main data concentration. Ultimately, correlation is most reliable if supported by a suite of different criteria.

Assessing the three models of partitioning Canton Schist FIAs

As all three models (Figs 6, 8 & 9) are consistent with the relative timing criteria, deciding between them depends upon whether orientation or textural criteria are more reliable as a means of distinguishing time-equivalent FIAs. As discussed above, the use of orientation as a criterion is unreliable in a clustered data set such as that recorded in the Canton Schist. The alternative is to use textural criteria and relative timing to correlate the FIAs, as in Model 1 (Fig. 6). This implies that the deflection plane coincident with the

core–rim boundary (e.g. Fig. 4a) developed at the same time in all samples collected over a > 10 km^2 area.

Bell & Johnson (1989) and Passchier & Trouw (1996) have proposed contrasting models for the development of deflection planes (termed truncation planes by Bell & Johnson) and accompanying change in the inclusion mineralogy. Bell & Johnson suggested the deflection planes represent the microstructural boundary between overprinting crenulation events. In contrast, Passchier & Trouw (1996) suggested that deflection planes represent the boundary between successive stages of garnet growth. In the Passchier & Trouw (1996) model, the decrease in quartz inclusions at the core–rim boundary represents a mica-rich strain cap that formed by pressure solution of quartz during the hiatus in garnet growth. It must be remembered that garnet rim growth may be diachronous over an area, but the deflection plane itself may represent the same crenulation cleavage recorded in many different samples. The relative age of the deflection plane thus may either represent the same crenulation or rotation event, or represent deflection surfaces of contrasting ages if garnet rim growth was diachronous. Similarly, the relative age of rim growth in different porphyroblasts may be either synchronous, diachronous over a regional gradient (e.g. syn-metamorphism temperature) or completely unrelated if the rim growth is tied to local critical conditions.

Within the Canton Schist, we propose that the deflection planes represent the same crenulation event in all samples. The evidence for this includes the consistent orientation of inclusion trail truncations at the core–rim boundary, the preservation of crenulations within the cores and rims of some porphyroblasts (e.g. figs 4 & 5 of Stallard & Hickey, 2001) and the consistent orientation of inclusion trail surfaces adjacent to the deflection surfaces (Fig. 10; Stallard & Hickey, 2001). Preference for Model 1 is further supported by the following three points. First, Model 1 accommodates natural variation in the orientation of geological structures and is consistent with the spread in FIA data recorded by Davis (1993). Given that the spread within each set is geologically reasonable, it is unnecessary to partition outlier data into a fourth set on the basis of orientation alone, as was done in Models 2 & 3. Second, The correlation of FIAs implicit in Model 1 is supported by the clockwise shift in orientation of many FIAs from Set 1 to Set 2 (Fig. 6b), and the consistent relationship between inclusion trail geometry and texture (Fig. 10). Finally, Model 1 requires fewer deformation events. This is consistent with explaining the data in the least complicated model. Preference for Model 1 does not change the minimum interpretation of three main FIA sets presented earlier. However it does suggest that the intrasample range in FIA orientations may be greater than previously thought (e.g. Bell *et al.*, 1998).

Implications for the use of FIAs as a geological tool

Given the subjectivity and uncertainty involved in the interpretation and correlation of inclusion trails, and the fact that FIA measurements do not represent discrete physical microstructures, it is more reasonable to treat FIA data as semiquantitative indicators of bulk trends rather than an exact measurement to be used for quantitative purposes. As mentioned earlier, presentation of FIAs as discrete orientations does not reflect

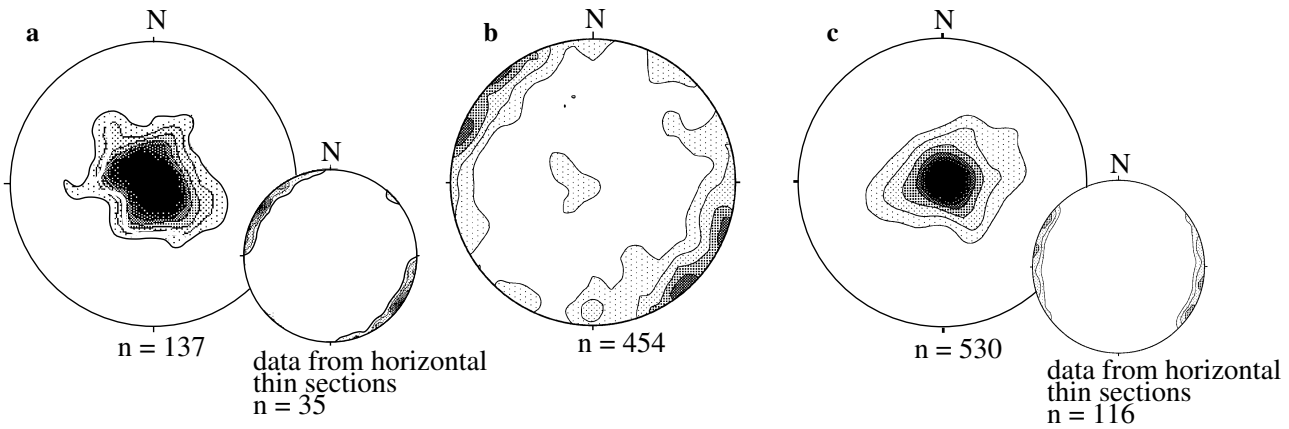

Fig. 10. Measurements of inclusion trail geometry either side of the core-rim transition in Canton Schist garnet. Truncations at the core–rim boundary have a steep pitch in all samples (a), while the pitches of inclusion trails within the core immediately adjacent to the core-rim transition are dominantly shallow (b) and inclusion trail pitches within the rim adjacent to the core–rim transition are predominantly steep (c). The pitches were measured in differently striking vertical thin sections from all samples of Canton Schist. Smaller stereoplots show data from horizontal thin sections (i.e. strike of measured surfaces). Thin sections were cut at 10–20° intervals around the compass (average 16 sections per sample). Data are counted on a sphere and smoothed as average of central point and eight adjacent points, with 4x weighting for central point. Contours represent concentration relative to uniform density, with lowest contour equal to 1 × uniform, and contour intervals of one (i.e. successive contours of 2x uniform, 3x, 4x, etc.). Modified from Stallard & Hickey (2001).

the nature of the raw data, and this degree of precision is probably not reproducible. Presentation of FIA data in the form of an estimate and interval of spread (i.e. 080 ± 10°) derived from a statistical analysis is more consistent with the nature of the raw data (i.e. inclusion trail curvature). Accordingly, FIA data are best used in geological investigations for tracking gross kinematic patterns. The uncertainties involved in the method of determining and correlating FIAs suggest the data may generally be less suited for quantitative investigations such as quantifying porphyroblast rotation or assessing fold mechanisms. Exceptions to this may occur where FIA data contain nonoverlapping sets of restricted distribution.

CONCLUSIONS

The minimum angular variation in FIA orientation within and between porphyroblasts in a sample is 30° in the Canton Schist, and this spread is proposed as typical for schistose rocks. Data presented as an estimate and confidence interval (e.g. 080 ± 15°) are representative of this spread in FIA orientations, and is more reproducible than data presented as a discrete value (e.g. 080°). Presentation of asymmetry plots provides an additional indicator of the reliability of the FIA data. Within a set of temporally related FIAs, it is likely that the majority of data (> 75% in the case of the Canton Schist) will cluster within a 60° interval. Smaller numbers of data may be oriented outside of this range, including at a high angle to the main data concentration.

Recognition of sets within FIA data depends upon the criteria chosen to correlate FIAs. Timing of FIAs relative to other FIAs from the core to rim of porphyroblasts is the most useful criteria for correlating FIAs, followed by inclusion trail textures and mineralogy, and distinctive patterns in the data. In populations of FIA data that contain a wide range of orientations, correlation on the basis of orientation is unreliable in the absence of additional criteria, as temporally related FIAs can have a large spread in orientations. In the Canton Schist, the spread in orientation of temporally related FIAs is typically 40–80°, but may be as much as 147°. Due to the intra- and intersample variation in FIA orientations and uncertainties in correlation, FIAs are best employed as semiquantitative indicators of bulk trends rather than an exact measurement to be used for quantitative purposes.

ACKNOWLEDGEMENTS

Critical reviews by A. Barker, R. Gibson, P. Hudleston, S. Johnson, C. Passchier and T. Bell are gratefully acknowledged. The idea for presenting data in the form of an asymmetry plot was originally suggested by D. Aerden. The first author acknowledges the support of a FRST Postdoctoral Fellowship at the University of Canterbury during the final stages of manuscript preparation.

SUPPLEMENTARY MATERIAL

Tables S1, S2 and S3 are available online from http://www.blackwellpublishing.com/products/journals/suppmat/JMG/JMG439/JMG439sm.htm.

REFERENCES

Bell, T. H., Forde, A. & Wang, J., 1995. A new indicator of movement direction during orogenesis: measurement technique and application to the Alps. *Terra Nova*, **7,** 500–508.

Bell, T. H. & Hickey, K. A., 1997. Distribution of pre-folding linear movement indicators around the Spring Hill Synform, Vermont: significance for mechanism of folding in this portion of the Appalachians. *Tectonophysics*, **274,** 275–294.

Bell, T. H., Hickey, K. A. & Upton, G. J. G., 1998. Distinguishing and correlating multiple phases of metamorphism across a multiply deformed region using the axes of spiral, staircase and sigmoidally curved inclusion trails in garnet. *Journal of Metamorphic Geology*, **16,** 767–794.

Bell, T. H. & Johnson, S. E., 1989. Porphyroblast inclusion trails: the key to orogenesis. *Journal of Metamorphic Geology*, **7,** 279–310.

Dallmeyer, R. D., 1978. $^{40}Ar/^{39}Ar$ incremental-release ages of horneblende and biotite across the Georgia inner Piedmont; their bearing on late Paleozoic-early Mesozoic tectonothermal history. *American Journal of Science*, **278,** 124–149.

Davis, B. K., 1993. Mechanism of emplacement of the Cannibal Creek Granite with special reference to timing and deformation history of the aureole. *Tectonophysics*, **224,** 337–362.

Edwards, A. W. F., 1972. *Likelihood: an Account of the Statistical Concept of Likelihood and its Application to Scientific Inference*. Cambridge University Press, Cambridge.

Fisher, N. I., 1993. *Statistical Analysis of Circular Data*. Cambridge University Press, Cambridge.

Hayward, N., 1990. Determination of early fold axis orientations within multiply deformed rocks using porphyroblasts. *Tectonophysics*, **179,** 353–369.

Hickey, K. A. & Bell, T. H., 1999. Behaviour of rigid objects during deformation and metamorphism: a test using schists from the Bolton syncline, Connecticut, USA. *Journal of Metamorphic Geology*, **17,** 211–228.

Johnson, S. E., 1993. Unravelling the spirals: a serial thin-section study and three-dimensional computer-aided reconstruction of spiral-shaped inclusion trails in garnet porphyroblasts. *Journal of Metamorphic Geology*, **11,** 621–634.

Johnson, S. E., 1999. Porphyroblast microstructures: a review of current and future trends. *American Mineralogist*, **84,** 1711–1726.

Jones, K. A., 1994. Progressive metamorphism in a crustal-scale shear zone: an example from the Leon region, northwest Brittany, France. *Journal of Metamorphic Geology*, **12,** 69–88.

Kohn, M. J., Orange, D. L., Spear, F. S., Rumble, D. & Harrison, T. M., 1992. Pressure, temperature and structural evolution of west-central New Hampshire: Hot thrusts over cold basement. *Journal of Petrology*, **33,** 521–566.

McConnell, K. I. & Abrams, C. E., 1984. Geology of the Greater Atlanta Region. *Georgia Geological Survey Bulletin*, **96,** 127p.

Passchier, C. W. & Trouw, R. A. J., 1996. *Microtectonics*. Springer-Verlag, Berlin.

Powell, D. & Treagus, J. E., 1967. On the geometry of S-shaped inclusion trails in garnet porphyroblasts. *Mineralogical Magazine*, **36,** 453–456.

Powell, D. & Treagus, J. E., 1970. Rotational fabrics in metamorphic minerals. *Mineralogical Magazine*, **37,** 801–814.

Rosenfeld, J. L., 1968. Garnet rotations due to the major Paleozoic deformations in southeast Vermont. In: *Studies of Appalachian Geology* (eds Zen, E.-an, et al.), pp. 185–202. Wiley Interscience, New York.

Schoneveld, C., 1979. The geometry and the significance of inclusion patterns in syntectonic porphyroblasts. *Unpublished PhD Thesis*, *University of Leiden, Leiden*.

Selverstone, J., Spear, F. S., Franz, G. & Morteani, G., 1984. High pressure metamorphism in the SW Tauen window, Austria: P-T paths from hornblende-kyanite-staurolite schists. *Journal of Petrology*, **25,** 501–531.

Stallard, A. R. & Hickey, K. A., 2001. Shear zone vs folding origin for spiral inclusion trails in the Canton Schist. *Journal of Structural Geology*, **23,** 1845–1864.

Received 27 November 2000; revision accepted 9 October 2002.